Original Article Open Access

Archives Of Breast Cancer

DOI: 10.32768/abc.6921483579-046

Evaluating Diagnostic Performance of Kaiser Score and BI-RADS in MRI Examination of Suspicious Breast Lesions: A Retrospective Study

Fahimeh Zeinalkhani[a,b], Peyman Kamali Hakim[a,b], Alisa Mohebbi[c], Zahra Shayegh[a], Zahra Moradi[c], Fatemeh Mahdavi Sabet[d], Ali Abdi[c], Amir Hosein heydari[a], Sharife Badr[a], Hadise Zeinalkhani[e], Fahimeh Azizinik[a], Fatemeh Shakki Katouli[a], Saeed Mohammadzadeh*[a,b]

[a]*Advanced Diagnostic and Interventional Radiology Research Center (ADIR), Tehran University of Medical Sciences, Imam Khomeini Hospital, Tehran, Iran*

[b]*Department of Radiology, Tehran University of Medical Sciences, Imam Khomeini Hospital, Tehran, Iran*

[c]*School of Medicine, Tehran University of Medical Sciences, Tehran, Iran.*

[d]*Department of Radiology, Iran University of Medical Sciences, Tehran, Iran, Faculty of Medicine, Tehran Medical Sciences Branch, Islamic Azad University, Tehran, Iran.*

[e]*Department of Radiology, Shahid Beheshti University of Medical Sciences, Tehran, Iran*

ARTICLE INFO

Received:
29 March 2026
Revised:
13 June 2026
Accepted:
15 June 2026

Keywords:
Breast Imaging Reporting and Data System, magnetic resonance imaging, background parenchymal enhancement, breast neoplasms, sensitivity and specificity

ABSTRACT

Background: The purpose of this study was to compare the diagnostic performance of the Kaiser score (KS) with Breast Imaging Reporting and Data System (BI-RADS) in breast magnetic resonance imaging (MRI) examination and to evaluate the impact of apparent diffusion coefficient (ADC), background parenchymal enhancement (BPE), and lesion type on its diagnostic efficacy.

Methods: This retrospective study included 259 patients who underwent breast MRI examination. Two blinded radiologists independently evaluated lesions using BI-RADS, KS, and ADC values. Histopathology served as the main reference standard. Diagnostic performance of BI-RADS, KS, ADC, and the combination of KS and ADC (Kaiser Plus) was evaluated. Subgroup analyses for mass/non-mass lesions and BPE were also performed.

Results: The area under the receiver operating characteristic curve (AUC) for BI-RADS, KS, ADC, and Kaiser Plus was 0.961 (95% CI, 0.931–0.980), 0.955 (95% CI, 0.924–0.976), 0.866 (95% CI, 0.807–0.913), and 0.959 (95% CI, 0.919–0.983), respectively. BI-RADS showed higher sensitivity (100% vs 88.2%) but lower specificity (75.3% vs 94.4%) than KS, resulting in comparable AUCs (DeLong $P = 0.65$). KS reduced unnecessary biopsies by 19.1% but missed 11.7% more malignancies. For mass lesions, KS achieved superior specificity (94.6% vs 75.7%) with minimal sensitivity trade-offs (93.0% vs 100%) compared with BI-RADS. Non-mass lesions posed challenges for all methods. In addition, KS performance did not differ significantly across BPE grades.

Conclusion: The KS showed comparable diagnostic value to BI-RADS, reducing unnecessary biopsies while providing consistent performance across lesion types. Our findings support the clinical utility of KS for breast MRI interpretation.

INTRODUCTION

Breast cancer is among the most common types of malignancy in women and is the second leading cause of female cancer mortality worldwide.[1] Magnetic resonance imaging (MRI) has proven to be a promising method in characterizing breast lesions, especially when conventional imaging methods such

***Address for correspondence:**
Saeed Mohammadzadeh,
Advanced Diagnostic and Interventional Radiology Research Center (ADIR), Tehran University of Medical Sciences, Imam Khomeini Hospital, Tehran, Iran;
Email: saeed.mohamadzadeh2001@gmail.com

as mammography and ultrasound are insufficient to definitively confirm or exclude malignant breast lesions.[2,3] MRI demonstrates the highest sensitivity among breast imaging modalities; however, it has lower specificity.[4] Moreover, the broad application of diverse MRI protocols enhances sensitivity but concurrently elevates false-positive rates, as the overlapping imaging features of benign and malignant lesions frequently preclude definitive differentiation. False-positive MRI findings can lead to unnecessary invasive procedures, an unfavorable harm-to-benefit ratio, and additional diagnostic workup prior to surgery.[5]

The standardized American College of Radiology Breast Imaging Reporting and Data System (BI-RADS) lexicon was developed to facilitate the evaluation of breast MRI images. Although BI-RADS lexicon criteria focus on morphological features and enhancement kinetics, the absence of a structured classification system, such as a flowchart, limits its practical application in confirming or excluding malignancy on breast MRI, particularly for less experienced radiologists.[6] Furthermore, lesions categorized as BI-RADS 4 are considered suspicious for malignancy and are typically recommended for biopsy. However, this category encompasses a wide malignancy probability, ranging from 2% to 95%.[7,8] Therefore, there is a need for more precise risk stratification.

The Kaiser score (KS), named after Werner Alois Kaiser, is a structured evidence-based decision tool derived directly from BI-RADS criteria and complex machine learning methods.[9] KS is a classification tree flowchart developed to support the evaluation of enhancing breast lesions on MRI. KS comprises 17 variables and incorporates 5 key diagnostic features: the spiculation sign, dynamic contrast enhancement curve type, lesion margins, internal enhancement pattern, and the presence of edema.[9] The proposed flowchart produces a diagnostic score on a scale from 1 to 11, where a threshold score above 4 indicates the need for biopsy. Literature has demonstrated high diagnostic accuracy, consistently reporting strong performance in distinguishing between benign and malignant breast lesions on MRI.[10–12] Moreover, evidence suggests that the KS provides greater diagnostic efficiency than the ACR BI-RADS system and effectively reduces the rate of unnecessary biopsies.[9]

Although the KS requires no postprocessing software or additional functional imaging, studies have explored combining it with quantitative data (eg, apparent diffusion coefficient [ADC]), clinical findings, or mammographic calcifications to enhance accuracy. While some studies showed no significant gains, others reported improvements using machine learning models, microcalcifications, or vascular assessment, emphasizing a combined modeling approach for optimal KS performance.[13]

Diffusion-weighted imaging (DWI) and ADC values derived from DWI data have been used in determining breast lesion characteristics. Benign lesions exhibit higher ADC values compared with malignant lesions; therefore, findings with high ADC values may help avoid unnecessary interventions.[14] An ADC cut point of $> 1.4 \times 10^{-3}$ mm^2/s has demonstrated a sensitivity of 100% in excluding malignancy.[15] Yet, previous studies integrating both indicators did not significantly improve the diagnostic performance of KS.[16,17]

Another factor influencing MRI interpretation is background parenchymal enhancement (BPE). Research has shown that a high level of BPE is related to breast cancer and can lead to false-negative or false-positive diagnoses.[18] Yet, the diagnostic performance of KS and BI-RADS depending on BPE has been investigated in a limited number of studies, which did not demonstrate a significant difference between KS and BI-RADS.[16]

In this study, we aimed to investigate the diagnostic performance of KS and assess the concordance of KS and BI-RADS. Additionally, given the potential complementary value of morphological and diffusion-based MRI, we aimed to investigate whether integrating ADC values with KS could improve diagnostic accuracy in evaluating breast lesions. Moreover, the effect of BPE on the diagnostic performance of KS was analyzed.

METHODS

Study design and patient population / study cohort

This retrospective study was conducted at Imam Khomeini Hospital Complex, a tertiary referral center with a large patient population. The institution's referral status improved the generalizability of our findings by reducing selection biases inherent in single-center studies. The institutional review board of this hospital approved the study protocol and waived the requirement for informed consent. All investigators signed confidentiality agreements to ensure data anonymity. We adhered to the ethical principles of the Declaration of Helsinki. The STARD (Standards for Reporting Diagnostic Accuracy Studies) checklist and supporting methodological details are available in the Supplementary Material.

All patient data were collected from medical records, picture archiving and communication systems (PACS), and pathology reports. This retrospective study reviewed 309 consecutive patients treated between 2021 and 2024. Inclusion criteria

comprised patients with suspicious breast lesions identified via ultrasound or mammography who subsequently underwent MRI examination. Exclusion criteria included patients with low-quality imaging studies; prior treatment with chemotherapy, radiotherapy, or hormone therapy; history of breast cancer or surgery; or lack of reference test results. The flowchart of patient selection is shown in Figure 1.

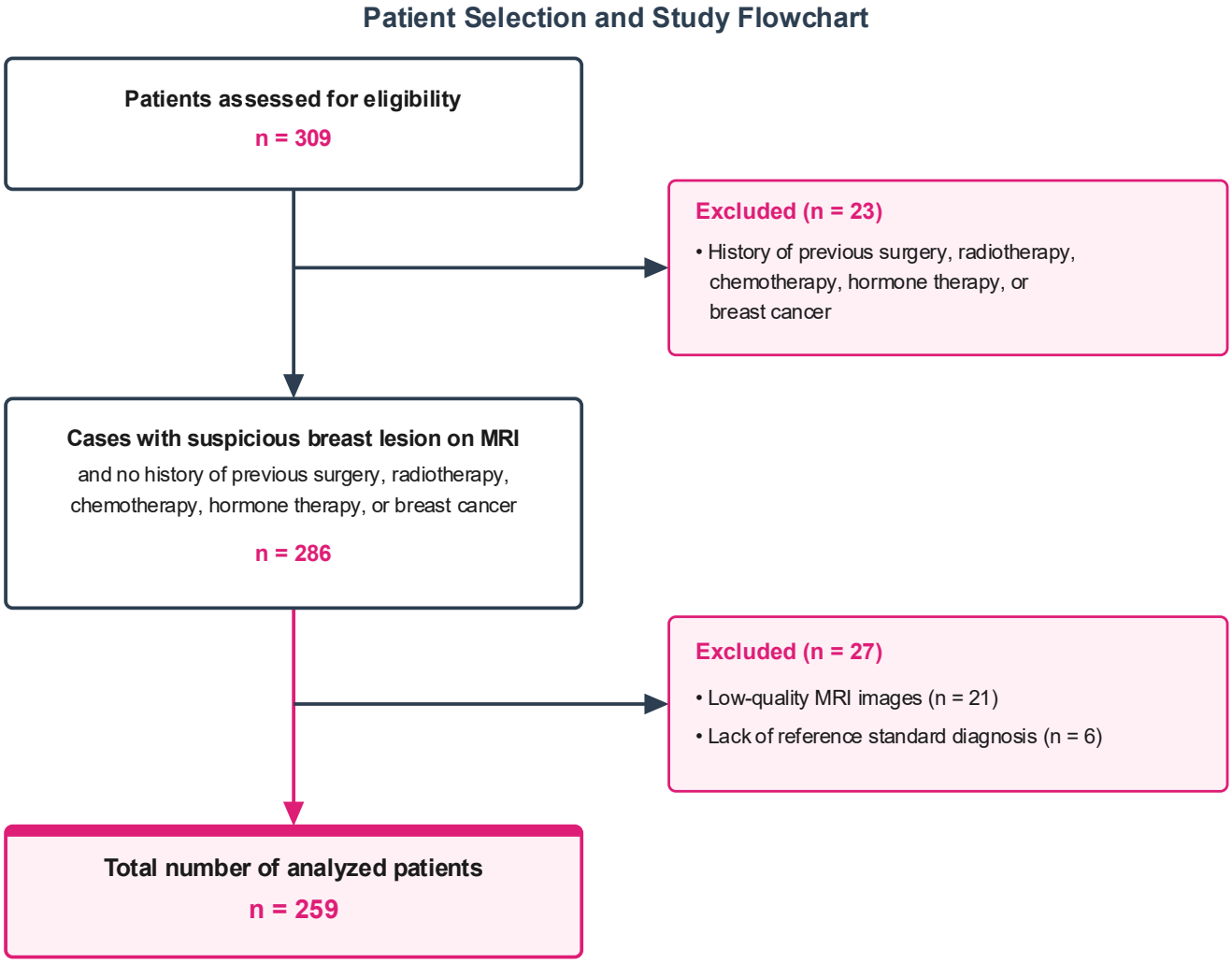

Figure 1. Flowchart of Patient Inclusion. Flow diagram illustrating patient screening, eligibility criteria, exclusions, and final study cohort selection.

Imaging acquisition

All MRI examinations were conducted with the patient in the prone position using a 1.5-T MRI scanner (General Electric Medical Systems) equipped with a dedicated bilateral 8-channel breast coil. The imaging protocol included axial T1-weighted sequences with a repetition time (TR) of 400 ms, echo time (TE) of 10 ms, bandwidth of 31.25 Hz/pixel, slice thickness of 5.0 mm, matrix size of 384 × 256, field of view (FOV) of 320 mm, and number of excitations (NEX) of 1. Axial short tau inversion recovery (STIR) sequences were acquired with TR/TE of 4500/63 ms, bandwidth of 62.5 Hz/pixel, slice thickness of 5.0 mm, matrix size of 320 × 256, FOV of 320 mm, and NEX of 1.

Dynamic contrast-enhanced (DCE) imaging was performed using a fat-suppressed axial 3D T1-weighted spoiled gradient-echo sequence after intravenous injection consisting of 1 precontrast baseline phase followed by 4 postcontrast phases for kinetic curve assessment. This standard 5-phase protocol (precontrast + 4 postcontrast) aligns with ACR BI-RADS recommendations to evaluate enhancement patterns (persistent, plateau, washout). Intravenous injection included 0.2 mmol/kg gadolinium-DTPA (Dotarem, Guerbet) followed by a 15-mL saline flush. Imaging parameters included TR/TE of 9/4 ms, bandwidth of 31.25 Hz/pixel, FOV of 320 mm, slice thickness of 2.0 mm, matrix size of 352 × 288, flip angle of 30°, and NEX of 1. DWI was

performed using an axial echo-planar sequence with spatial fat suppression, 10 minutes postcontrast injection. DWI parameters included TR/TE of 7700/89 ms, FOV of 380 mm, flip angle of 90°, matrix size of 192 × 192, slice thickness of 5.0 mm, NEX of 4, and b-values of 0, 400, and 800 s/mm^2.

Data analysis

All MRI examinations were evaluated independently by 2 radiologists with 7 and 20 years of experience, respectively. Radiologists were blinded to clinical and histological information as well as other readers' assessments. To minimize recall bias and interpretation overlap, an interval of 1 month was enforced between the interpretation of the KS and the BI-RADS score. Each lesion was scored based on the MRI BI-RADS classification system and then reevaluated using the KS. BPE was categorized using a standardized 4-point qualitative scale assessing fibroglandular tissue enhancement patterns. Grade 1 (minimal) represented ≤ 25% enhancement with faint, patchy patterns barely different from baseline, while grade 2 (mild) showed 25% to 50% nonconfluent enhancement. Grade 3 (moderate) demonstrated 50% to 75% confluent enhancement with visible vascularity, features that can overlap with those of small lesions, and grade 4 (severe) exhibited > 75% dense, confluent enhancement markedly obscuring parenchymal architecture with prominent vascularity.

For enhancing lesions, the 2 radiologists categorized findings according to the BI-RADS MRI lexicon as either mass or non-mass enhancement. Masses were regarded as 3-dimensional space-occupying lesions with convex borders and specific morphological features evaluated in 3 planes. Non-mass enhancements were characterized as areas of enhancement that, unlike masses in morphology, displayed distributed patterns including focal, linear, ductal, segmental, regional, multiple regions, or diffuse. Discrepancies in initial reader evaluations were addressed through collaborative discussion to achieve final image interpretation by consensus for each case.

ADC values for each lesion were assessed using ADC maps transferred to a specialized workstation. Two radiologists independently identified and outlined regions of interest (ROIs) on the maps guided by anatomical details from DCE-MRI. These ROIs were restricted to solid tumor components, taking care to exclude areas showing necrosis, cystic changes, or hemorrhage. Following ROI placement, the ADC values were extracted. The final ADC value for each lesion was calculated as the average of the 2 radiologists' measurements. Three clinical examples and comparisons of imaging findings of breast lesions and histopathological analysis are presented in Figures 2, 3, and 4.

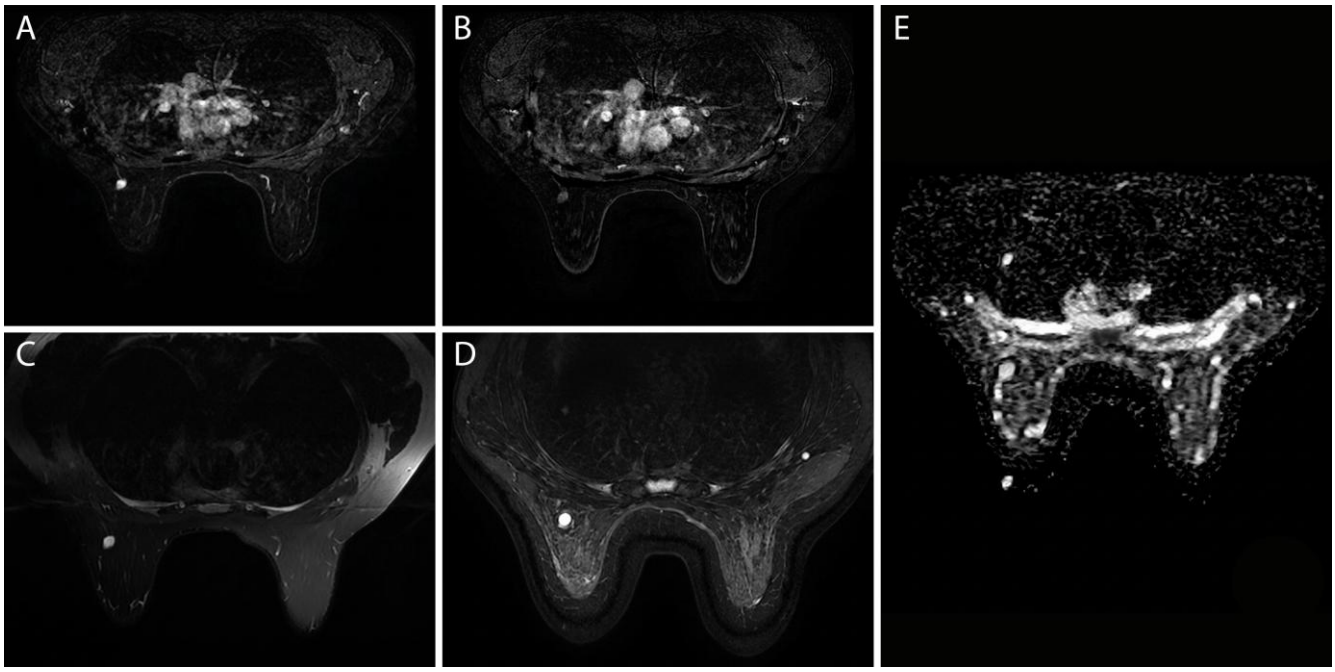

Figure 2. Breast MRI Findings of a Benign Mass in a 48-Year-Old Woman. A, Early subtraction phase image demonstrating heterogeneous progressive enhancement. B, Late subtraction phase image. C, T2-weighted image. D, Diffusion-weighted image (DWI). E, Corresponding apparent diffusion coefficient (ADC) map showing a mean ADC value of 1.607×10^{-3} mm^2/s. The lesion was categorized as Kaiser score 3 (benign) and BI-RADS category 4 (suspicious). Histopathological evaluation confirmed a fibroadenoma.

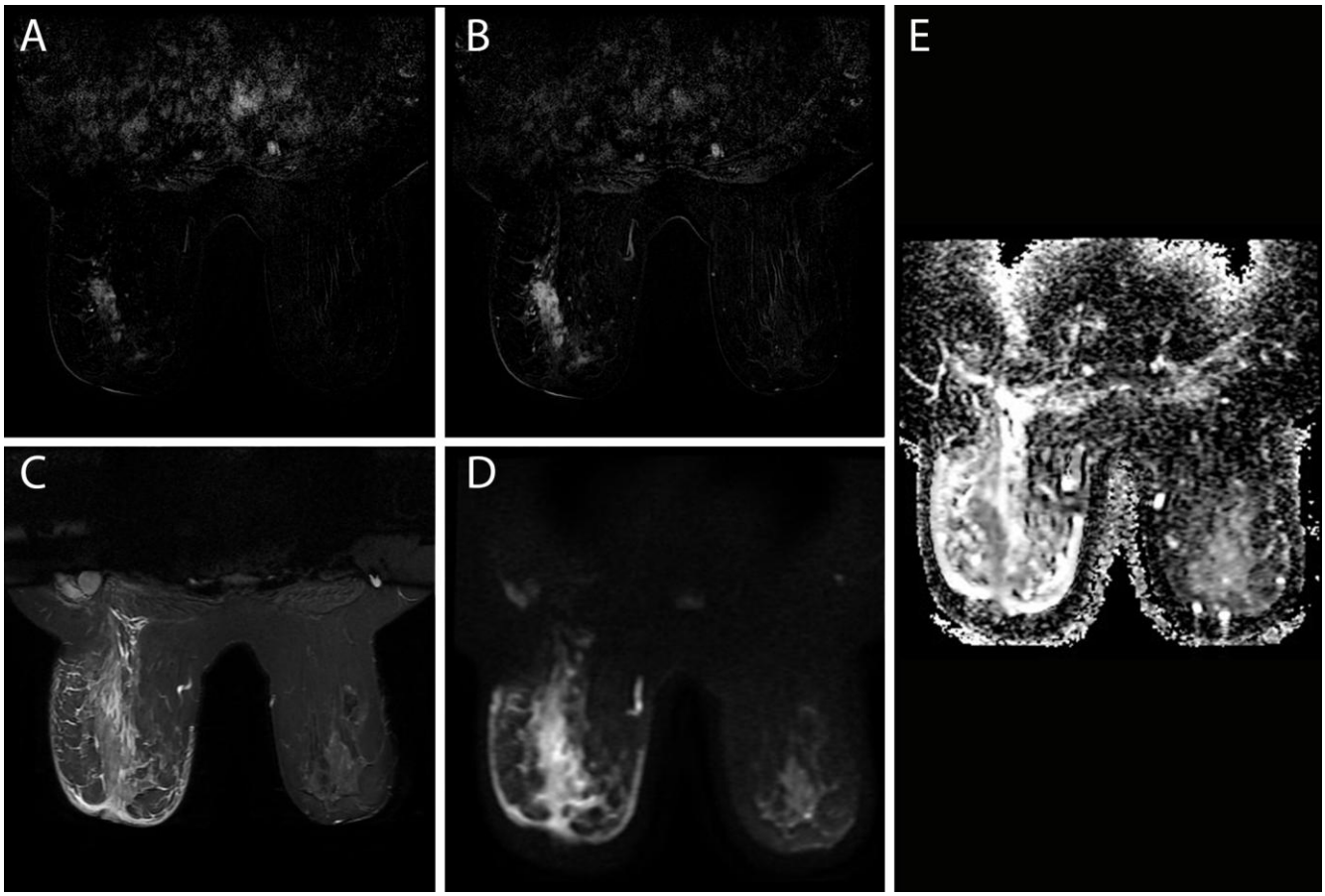

Figure 3. Breast MRI Findings of Non-Mass Enhancement in a 53-Year-Old Woman. A, Early subtraction image showing heterogeneous segmental non-mass enhancement in the left breast with areas of progressive enhancement. B, Late subtraction image. C, T2-weighted image showing marked diffuse edema. D, Diffusion-weighted image (DWI). E, Apparent diffusion coefficient (ADC) map showing an ADC value of 1.230×10^{-3} mm^2/s. Note the presence of enlarged ipsilateral axillary lymph nodes. The lesion was assigned a Kaiser score of 6 and a BI-RADS category of 4. Histopathological examination confirmed invasive ductal carcinoma.

Statistical analysis

Statistical analysis was performed using MedCalc (version 22.107, MedCalc Software Ltd) and Stata 18.0 (StataCorp LLC). Diagnostic performance values, including sensitivity, specificity, positive likelihood ratio (PLR), and negative likelihood ratio (NLR), were calculated for BI-RADS, KS, ADC, and Kaiser Plus. True positives (TP), true negatives (TN), false positives (FP), and false negatives (FN) were determined for both BI-RADS and KS categories. For BI-RADS, scores > 3 were considered malignant, while scores ≤ 3 indicated benign lesions. A lesion was counted as TP if BI-RADS classified it as malignant and histopathology confirmed malignancy. If both BI-RADS and histopathology indicated a benign lesion, it was considered a TN lesion. Cases where BI-RADS suggested malignancy but pathology showed benign findings were labeled FPs, and lesions misclassified as benign by BI-RADS but proven to be malignant were counted as FNs.

The same approach was applied to the Kaiser score, where scores > 4 were classified as malignant. TPs were defined as lesions classified as malignant by the KS and confirmed by histopathology. TNs were lesions classified as KS-benign and histopathologically benign. FPs were lesions misclassified as malignant but benign on histopathology, whereas FNs were lesions misclassified as benign but malignant on histopathology. For ADC, the optimal threshold was determined using the Youden index, which maximizes the sum of sensitivity and specificity. Receiver operating characteristic (ROC) curves were plotted, and their AUCs were calculated. The DeLong test was used to compare AUCs. Subgroup analyses were performed based on BPE grade and lesion type. Kaiser Plus was defined as a logistic regression model combining KS and ADC, with sensitivity and specificity derived using the Youden index. Pairwise correlation between all study variables was assessed using the Pearson correlation coefficient (r). Probability plots for BPE provided complementary analysis showing the probability of malignancy across the spectrum of observed values. Statistical significance was set at $P < 0.05$.

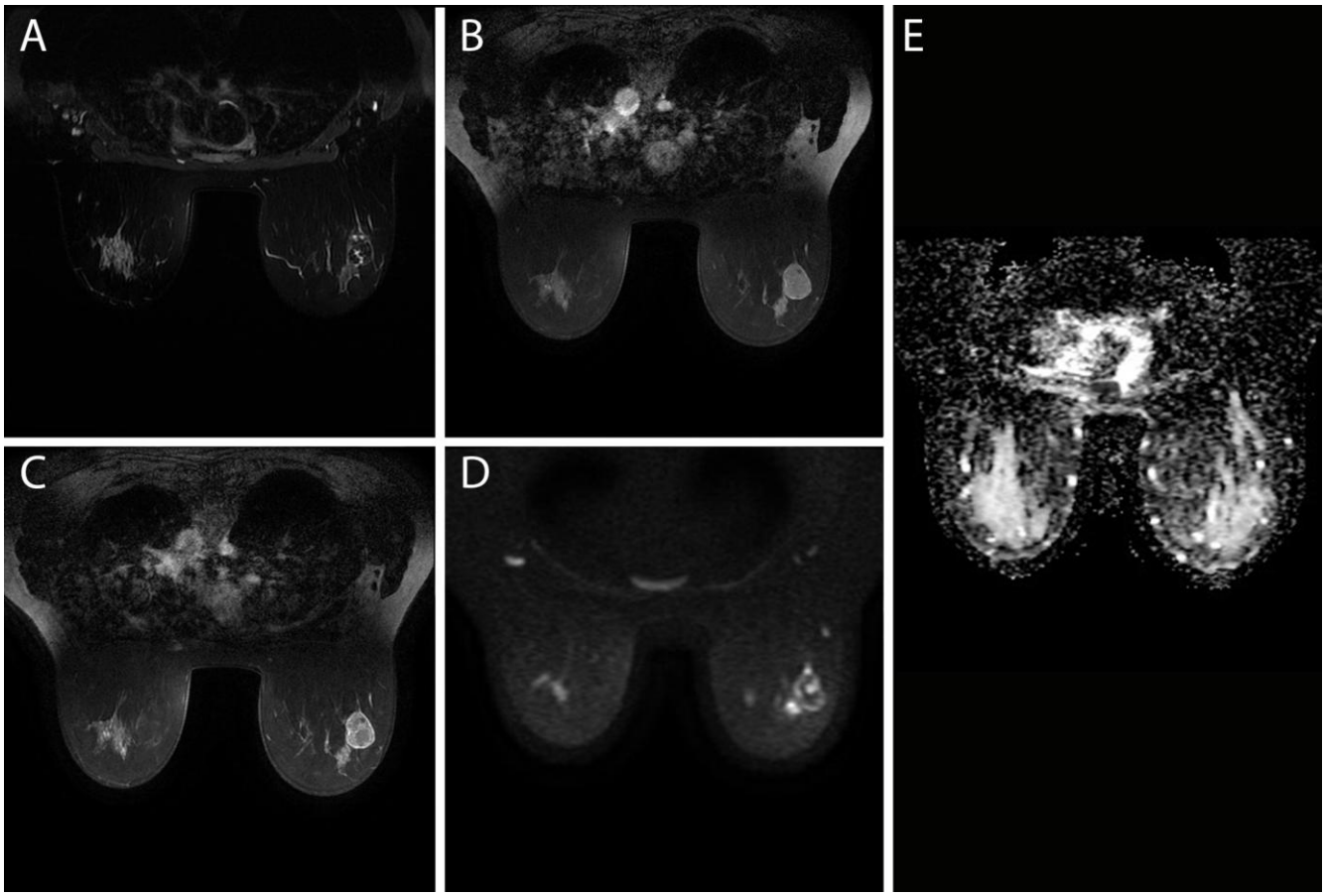

Figure 4. Breast MRI Findings of a Circumscribed Oval Mass in the Right Breast of a Patient with Invasive Ductal Carcinoma. A, Axial T2-weighted image. B, Postcontrast dynamic T1-weighted image showing a circumscribed oval mass with rim enhancement and heterogeneous progressive enhancement kinetics. C, Delayed-phase postcontrast T1-weighted image. D, Axial diffusion-weighted image (DWI). E, Axial apparent diffusion coefficient (ADC) map showing a mean ADC value of 1.800×10^{-3} mm^2/s with small focal areas of restricted diffusion. The lesion was categorized as Kaiser score 1 but classified as BI-RADS category 4. Histopathological examination confirmed invasive ductal carcinoma.

RESULTS

Patient and lesion characteristics

A total of 259 patients with 284 breast lesions were included in the study. Overall, 236 patients (91.1%) presented with a single lesion, 21 patients (8.1%) had 2 lesions, and 2 patients (0.8%) had 3 lesions. Among the 284 lesions, 89 (31.3%) were confirmed as benign and 195 (68.7%) were malignant. Furthermore, 232 lesions (81.7%) were mass lesions and 52 (18.3%) were non-mass enhancements. Among the 284 lesions included, 223 (78.6%) had a reference standard verified by biopsy, while 61 (21.4%) were confirmed by follow-up imaging.

The mean age of patients was 45.8 years (95% CI, 44.5–47.2) and did not differ significantly between patients with benign and malignant lesions ($P = 0.83$). Lesion size averaged 28.2 mm (95% CI, 25.5–30.9 mm), with no significant difference between benign and malignant lesions ($P = 0.08$).

Among the lesions, BI-RADS 3 lesions (67/284, 23.6%) were all classified as KS < 5 (benign; 100%). BI-RADS 4 lesions (84/284, 29.6%) comprised 34 KS < 5 (40.5%) and 50 KS > 4 (malignant; 59.5%). BI-RADS 5 lesions (127/284, 44.7%) included 6 KS < 5 (4.7%) and 121 KS > 4 (95.3%). All BI-RADS 6 lesions (6/284, 2.1%) were classified as KS > 4 (malignant; 100%).

Interclassifier correlations and pairwise concordance

Pearson correlation analysis revealed strong positive correlations between imaging classifiers and pathological outcomes (Figure 5A). BI-RADS demonstrated the highest correlation with pathology ($r = 0.81$, $P < 0.001$), followed by KS ($r = 0.75$, $P < 0.001$). The correlation between BI-RADS and KS was also substantial ($r = 0.75$, $P < 0.001$), indicating good concordance despite their different diagnostic thresholds. These strong correlations underscore the validity of both classification systems in breast lesion characterization.

ADC values showed significant negative correlations with both imaging classifiers: BI-RADS ($r = -0.44$, $P < 0.001$) and KS ($r = -0.48$, $P < 0.001$). This confirms the expected pattern whereby malignant

lesions exhibit lower ADC values than benign lesions. BPE demonstrated a significant positive correlation with the KS ($r = 0.16$, $P = 0.007$), while showing no significant association with BI-RADS ($r = 0.09$, $P = 0.15$).

This differential correlation pattern indicates that the pathophysiological concepts underlying background parenchymal enhancement, although showing only a trivial correlation, are explicitly incorporated into the KS algorithm but remain unaccounted for in the traditional BI-RADS assessment framework.

Lesion type showed differential correlations across imaging systems, with a significant negative correlation with BI-RADS ($r = -0.14$, $P = 0.02$) and a borderline significant association with the KS ($r = -0.12$, $P = 0.05$). This suggests that the type of enhancement (mass vs non-mass enhancement) influences diagnostic scoring differently between the two systems, with BI-RADS showing stronger dependence on type of enhancement categorization. The negative correlation indicates that non-mass lesions tend to receive lower diagnostic scores, reflecting the inherent challenges in characterizing these lesions regardless of the classification system employed.

Overall diagnostic performance of different imaging classifiers

For BI-RADS, the AUC reached 0.961 (95% CI, 0.931–0.980), demonstrating robust discriminative capacity. Sensitivity and specificity were 100% (95% CI, 98.1%–100%) and 75.3% (95% CI, 65.0%–83.8%), respectively.

The KS exhibited a more balanced profile, with an AUC of 0.955 (95% CI, 0.924–0.976), sensitivity of 88.2% (95% CI, 82.8%–92.4%), and specificity of 94.4% (95% CI, 87.4%–98.2%). The KS reduced unnecessary biopsies by correctly reclassifying BI-RADS false positives. The high sensitivity of BI-RADS came at the cost of 19.1% more false positives than KS, resulting in unnecessary biopsies for 17 benign lesions. The 19.1% reduction in unnecessary biopsies provided by KS offered clinical benefit despite a modest decrease in sensitivity, which resulted in 11.7% (n = 23) more missed cancers compared with BI-RADS. The difference in AUC between KS and BI-RADS was not statistically significant (DeLong $P = 0.65$).

Malignant lesions showed a mean ADC value of 0.98×10^{-3} mm^2/s (95% CI, 0.95–1.02×10^{-3} mm^2/s), while benign lesions showed a mean ADC value of 1.37×10^{-3} mm^2/s (95% CI, 1.23–1.50×10^{-3} mm^2/s) ($P < 0.001$). ADC values alone showed comparable performance to the KS, with an AUC of 0.866 (95% CI, 0.807–0.913). At a threshold of $\leq 1.18 \times 10^{-3}$ mm^2/s, sensitivity and specificity were 83.9% (95% CI, 77.1%–89.3%) and 82.6% (95% CI, 61.2%–95.0%), respectively.

Integrating ADC into the KS (Kaiser Plus) yielded an AUC of 0.959 (95% CI, 0.919–0.983). Sensitivity and specificity values at the optimal cut point were 96.1% (95% CI, 91.8%–98.6%) and 87.0% (95% CI, 66.4%–97.2%). DeLong tests confirmed no statistically significant improvement over standalone KS ($P > 0.05$). Summarized diagnostic values and ROC curves are displayed in Table 1 and Figure 5B.

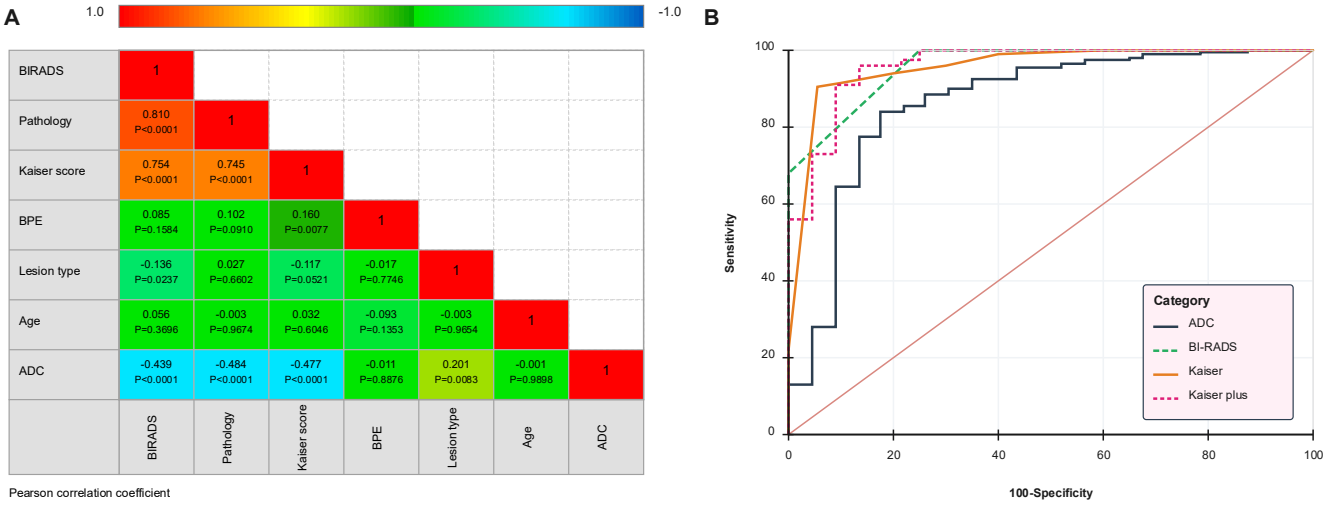

Figure 5. Correlation Matrix and Overall Receiver Operating Characteristic (ROC) Curves. A, Heatmap of pairwise correlation coefficients among imaging classifiers, clinicopathological features, and study measures. B, ROC curves evaluating the diagnostic performance of BI-RADS, Kaiser score, apparent diffusion coefficient (ADC), and Kaiser Plus in predicting breast malignancy across all 284 lesions.

Table 1. Diagnostic Performance Metrics of BI-RADS, Kaiser Score, ADC, and Kaiser Plus Stratified by Lesion Type

Lesion Type	Method	Sensitivity	Specificity	AUC
Overall	BI-RADS	195/195 (100%)	67/89 (75.3%)	0.961 (95% CI = 0.931 to 0.980)
	Kaiser	172/195 (88.2%)	84/89 (94.4%)	0.955 (95% CI = 0.924 to 0.976)
	ADC	130/155 (83.9%)	19/23 (82.6%)	0.866 (95% CI = 0.807 to 0.913)
	Kaiser Plus	149/155 (96.1%)	20/23 (87.0%)	0.959 (95% CI = 0.919 to 0.983
Mass	BI-RADS	158/158 (100%)	56/74 (75.7%)	0.973 (95% CI = 0.943 to 0.990)
	Kaiser	147/158 (93.0%)	70/74 (94.6%)	0.964 (95% CI = 0.932 to 0.984)
	ADC	121/134 (90.3%)	18/20 (90.0%)	0.927 (95% CI = 0.873 to 0.962)
	Kaiser Plus	129/134 (96.3%)	18/20 (90.0%)	0.979 (95% CI = 0.942 to 0.995)
Non-mass	BI-RADS	37/37 (100%)	11/15 (73.3%)	0.903 (95% CI = 0.788 to 0.967)
	Kaiser	25/37 (67.6%)	14/15 (93.3%)	0.875 (95% CI = 0.754 to 0.950)
	ADC	7/21 (33.3%)	3/3 (100%)	0.675 (95% CI = 0.455 to 0.850)
	Kaiser Plus	18/21 (85.7%)	2/3 (66.7%)	0.698 (95% CI = 0.479 to 0.867)

ADC, apparent diffusion coefficient; AUC, area under the receiver operating characteristic curve; BI-RADS, Breast Imaging Reporting and Data System; CI, confidence interval.

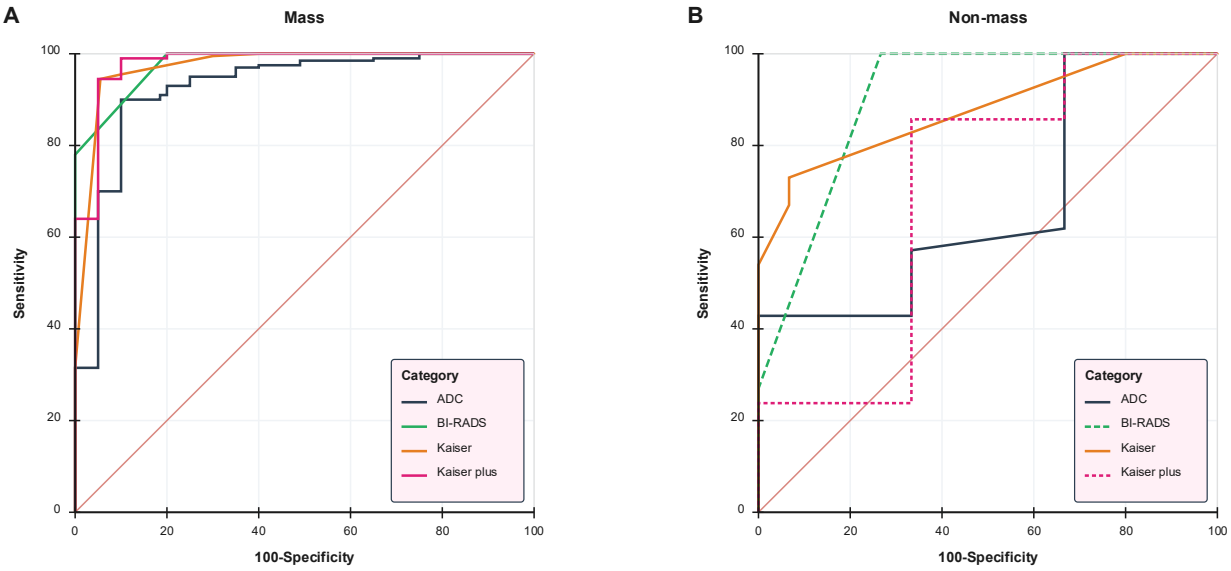

Figure 6. Subgroup Receiver Operating Characteristic (ROC) Curves Stratified by Lesion Type. A, ROC curves of BI-RADS, Kaiser score, apparent diffusion coefficient (ADC), and Kaiser Plus in mass lesions (n = 232). B, ROC curves of BI-RADS, Kaiser score, ADC, and Kaiser Plus in non-mass enhancement lesions (n = 52).

Performance in mass and non-mass lesions

In the evaluation of mass lesions (n = 232) (Figure 6A), BI-RADS demonstrated exceptional diagnostic performance with an AUC of 0.973 (95% CI, 0.943–0.990), achieving 100% sensitivity (95% CI, 97.7%–100%) and 75.7% specificity (95% CI, 64.3%–84.9%). The KS showed comparable accuracy, with an AUC of 0.964 (95% CI, 0.932–0.984), sensitivity of 93.0% (95% CI, 87.9%–96.5%), and superior specificity of 94.6% (95% CI, 86.7%–98.5%). ADC values alone achieved an AUC of 0.927 (95% CI, 0.873–0.962), with sensitivity and specificity of 90.3% (95% CI, 84.0%–94.7%) and 90.0% (95% CI, 68.3%–98.8%), respectively. Integration of ADC into the KS (Kaiser Plus) yielded the highest AUC in this subgroup at 0.979 (95% CI, 0.942–0.995), with sensitivity of 96.3% (95% CI, 91.5%–98.8%) and specificity matching standalone ADC (90.0%; 95% CI, 68.3%–98.8%).

Diagnostic performance declined across all methods for non-mass lesions (n = 52) (Figure 6B). BI-RADS maintained high sensitivity (100%; 95% CI, 90.5%–100%) but lower specificity (73.3%; 95% CI, 44.9%–92.2%), resulting in an AUC of 0.903 (95% CI, 0.788–0.967). The KS exhibited reduced sensitivity (67.6%; 95% CI, 50.2%–82.0%) but improved specificity (93.3%; 95% CI, 68.1%–99.8%), yielding an AUC of 0.875 (95% CI, 0.754–0.950). ADC values performed poorly in this subgroup, with an AUC of 0.675 (95% CI, 0.455–0.850), sensitivity of 33.3% (95% CI, 14.6%–57.0%), and specificity of 100% (95% CI, 29.2%–100%). Kaiser Plus showed marginal improvement over ADC alone (AUC = 0.698; 95% CI, 0.479–0.867),

though without statistical significance. DeLong tests revealed no significant differences in AUCs between BI-RADS, KS, and Kaiser Plus for either mass or non-mass lesions ($P > 0.05$). Summarized diagnostic values for mass and non-mass lesions are displayed in Table 1.

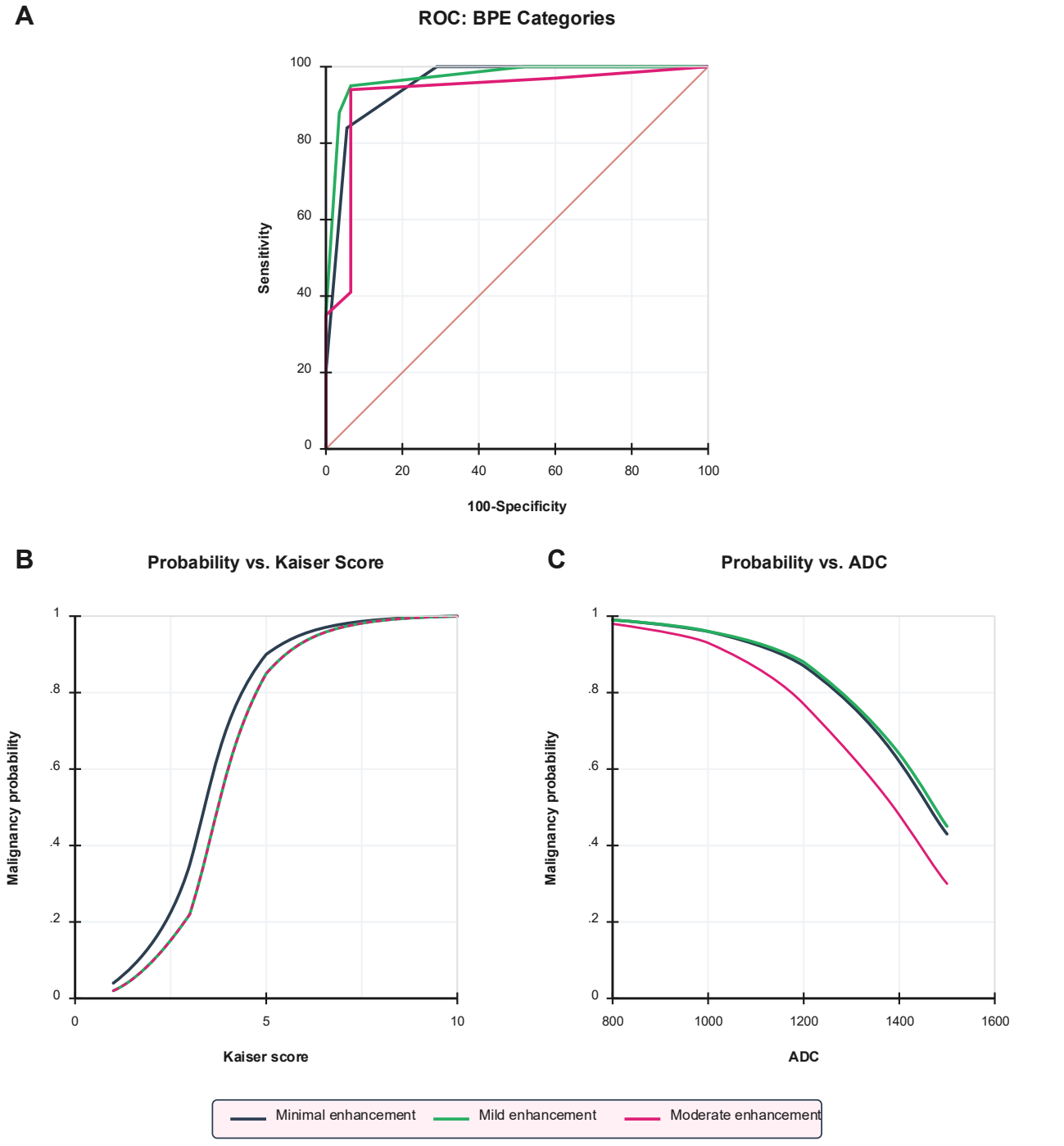

Figure 7. Diagnostic Performance and Malignancy Probability Plots Across Background Parenchymal Enhancement (BPE) Grades. A, Receiver operating characteristic (ROC) curves for the Kaiser score stratified by BPE grade. B, Malignancy probability plots for the Kaiser score across BPE grades. C, Malignancy probability plots for apparent diffusion coefficient (ADC) values across BPE grades.

Effect of background parenchymal enhancement

The influence of BPE on diagnostic accuracy was analyzed across 277 lesions, with BPE grades distributed as follows: 101 minimal (36.4%), 115 mild (41.5%), 50 moderate (18.0%), and 11 severe/marked (4.0%). The marked BPE grade was assessed descriptively but was not included in statistical subgroup comparisons due to insufficient sample size.

For the KS, the AUC remained similar across all evaluated grades of BPE, ranging from 0.932 to 0.974 ($P > 0.05$) (Table 2). Figures 7A and 7B display the ROC and probability plots for the performance of KS across different BPE grades.

Table 2. Area Under the Receiver Operating Characteristic Curve for Kaiser Score and Kaiser Plus Across Background Parenchymal Enhancement Grades

Imaging classifier	BPE grade	AUC (95% CI)
Kaiser score	Minimal	0.954 (0.892–0.985)
	Mild	0.974 (0.925–0.994)
	Moderate	0.932 (0.824–0.984)
Kaiser Plus	Minimal	0.982 (0.906–1.000)
	Mild	0.982 (0.922–0.999)
	Moderate	0.880 (0.712–0.968)

AUC, area under the receiver operating characteristic curve; BPE, background parenchymal enhancement; CI, confidence interval.

For Kaiser Plus scoring, the AUC also remained stable across BPE grades, ranging from 0.880 to 0.982 ($P > 0.05$). Figure 7C displays the probability plot for performance of ADC across different BPE grades. These findings confirm the limited impact of BPE on structured diagnostic algorithms such as the Kaiser and Kaiser Plus scores.

DISCUSSION

Our study demonstrates that the KS represents a highly effective diagnostic tool for breast MRI interpretation, offering comparable diagnostic accuracy to the established BI-RADS classification system while providing superior specificity in distinguishing benign from malignant breast lesions. Our findings corroborate previous international validation studies demonstrating the robust performance of the KS across diverse clinical settings and patient populations.[11,19]

The exceptional diagnostic performance observed with both BI-RADS and Kaiser systems in our study aligns with established literature demonstrating the superior sensitivity of breast MRI for cancer detection.[4] The BI-RADS system achieved 100% sensitivity in our study, consistent with meta-analyses reporting high sensitivities for breast MRI.[20,21] However, this high sensitivity came at the cost of reduced specificity, resulting in unnecessary biopsies for nearly a quarter of benign lesions. This finding underscores a fundamental challenge in breast imaging, where maximizing cancer detection must be balanced against the clinical and psychological burden of false-positive results. It is noteworthy that we assessed KS performance at the lesion level, assuming independence despite potential clustering from multiple lesions per patient. However, patient-level analysis was not conducted to avoid data loss from excluding smaller lesions in patients.

The KS demonstrated a balanced diagnostic profile, achieving excellent sensitivity while substantially improving specificity compared with BI-RADS. With a specificity exceeding 94% and a sensitivity of nearly 88%, the KS substantially reduced the rate of false positives and unnecessary biopsies compared with BI-RADS. This reduction in unnecessary interventions is clinically significant, as it minimizes patient anxiety and morbidity while optimizing health care resources—addressing primary limitations of breast MRI in clinical practice.[22] The improved specificity observed with the KS reflects its evidence-based algorithmic approach, which systematically incorporates morphological and kinetic features validated across multiple studies.[19] These results are in line with a meta-analysis reporting that the KS consistently outperforms BI-RADS in specificity, with pooled specificity rates approximately 24% higher than BI-RADS while maintaining comparable overall diagnostic accuracy.[13]

In our study, the KS correctly reclassified a significant proportion of BI-RADS 4 false positives, directly reducing the number of benign lesions subjected to biopsy. Cancers missed by KS compared with BI-RADS mostly occurred in small lesions (≤ 2 cm), cases with microcalcifications, or foci/non-mass enhancements with subtle features, where structured criteria may underweight atypical kinetics or BPE overlap. Previous research attributes such misses to the emphasis of KS on morphology over diffuse patterns and lower weighting for certain low-grade tumors that mimic benign findings.[13] Notably, conceptual overlap exists between the KS and BI-RADS lexicon, as KS was derived directly from BI-RADS descriptors and both utilize similar MRI features. This likely limited the observed performance differences, consistent with our results showing superior KS performance yet highly similar metrics across KS, KS-plus, and BI-RADS. Furthermore, the structured, algorithmic nature of the KS enhances diagnostic consistency and inter-reader agreement, particularly among less experienced radiologists. While BI-RADS requires substantial clinical judgment and experience, the KS provides an evidence-based decision tree that systematically incorporates key imaging features, leading to improved reproducibility and reliability across different users and clinical settings.[12,23]

The integration of ADC values into the KS framework (Kaiser Plus) yielded marginal improvements in diagnostic performance that did not reach statistical significance. This finding contrasts

with some previous studies suggesting the complementary value of DWI in breast lesion characterization.[15,24,25] However, our results align with recent investigations demonstrating that while ADC values provide valuable quantitative information, their integration with established morphological scoring systems may not significantly enhance overall diagnostic accuracy.[4,26] Morphological and kinetic features captured by structured systems such as the KS may already encapsulate critical diagnostic information, limiting the additive value of ADC integration.[27]Nevertheless, given these modest additive values and the single-center nature of our data, prospective validation of the Kaiser Plus approach remains essential to confirm its clinical utility.

The limited incremental benefit of Kaiser Plus may also stem from technical and biological factors influencing ADC reproducibility. Variations in DWI protocols (eg, b-value selection, postcontrast timing, and ROI placement) introduce measurement variability that can obscure subtle diagnostic gains.[28] Furthermore, overlapping ADC ranges between specific malignant subtypes (eg, mucinous carcinomas, DCIS) and benign lesions complicate threshold-based stratification.[29] For non-mass enhancements, ADC performance declined markedly (AUC = 0.675), reflecting inherent challenges in characterizing these lesions across imaging modalities. The structured Kaiser algorithm's insensitivity to ADC integration underscores its robustness against technical variability, making it preferable for standardized reporting. Nevertheless, ADC thresholds remain valuable adjuncts in scenarios requiring nuanced risk assessment, such as high-risk screening or in patients with contraindications to contrast administration.[28,30] Future protocols could prioritize concurrent but separate reporting of KS and ADC values, allowing clinicians to weigh morphological and diffusion-based data dynamically based on lesion type and clinical context.

The differential performance observed between mass and non-mass lesions represents a crucial finding with significant clinical implications. All diagnostic systems demonstrated superior performance for mass lesions compared with non-mass enhancements. This differential performance has been consistently reported in the literature and reflects overlapping features between benign and malignant non-mass enhancements.[25,31] The KS and ADC values may struggle with non-mass enhancements due to their diffuse, heterogeneous patterns, which lack distinct morphologic margins and internal enhancement characteristics that KS evaluates systematically.[25] In our study, the KS achieved excellent diagnostic accuracy with high specificity for mass lesions, confirming its utility in reducing unnecessary biopsies while maintaining high cancer detection rates. The superior specificity of the KS for mass lesions likely reflects the systematic evaluation of morphological features such as margins and internal enhancement patterns, which are particularly discriminative for mass-like lesions.[32] The reduced sensitivity of the KS for non-mass lesions, while noteworthy, must be interpreted within the broader context of breast MRI performance. Non-mass enhancements represent a heterogeneous group of findings that can be challenging to characterize even with comprehensive multiparametric imaging.[33,34] Future strategies could incorporate advanced texture analysis or radiomics features tailored to non-mass patterns, potentially combined with machine learning models trained specifically on these lesions to improve sensitivity without compromising specificity. The maintained high specificity of the KS for non-mass lesions suggests that when the algorithm indicates malignancy, the positive predictive value remains high, supporting biopsy recommendations.

To our knowledge, our study is among the first comprehensive evaluations of KS performance across varying BPE grades. Our analysis provides evidence that the KS maintains consistent accuracy across different BPE levels. This finding is particularly important given the growing recognition of BPE as both a potential confounding factor in breast MRI interpretation and an independent marker of breast cancer risk.[18,35,36] The consistent performance of the KS across BPE categories suggests that the structured algorithmic approach effectively accounts for background enhancement variations that might otherwise influence subjective interpretation. The positive correlation observed between background parenchymal enhancement and KS likely reflects the explicit incorporation of background enhancement considerations within the Kaiser algorithm. This systematic accounting for background parenchymal enhancement represents an advantage over traditional BI-RADS assessment, where the impact of background enhancement on diagnostic decisions may be more variable and reader-dependent. However, the marked BPE subgroup was too small for a separate diagnostic performance analysis, as it included only 11 lesions, limiting meaningful comparison.

Future research should focus on refining the KS framework to address persistent challenges, such as its reduced sensitivity for non-mass lesions. Integrating novel biomarkers, including vascular assessment metrics like increased ipsilateral breast vascularity or the adjacent vessel sign, could enhance

diagnostic accuracy for these complex lesions as preliminary studies report AUC improvements from 0.725 to 0.793 in non-mass subgroups when combining KS with vascular evaluation.[37] Similarly, exploring synergies with advanced imaging techniques, such as ultrafast dynamic MRI or synthetic contrast-enhanced protocols, may further improve lesion characterization while reducing scan time.[4,38] The growing role of artificial intelligence (AI) in breast MRI presents another promising avenue, with AI-driven tools showing potential to automate KS calculations, standardize ADC measurements, and predict histopathological subtypes.[39] Wider adoption of the KS in screening populations, particularly for high-risk women and those with dense breasts could maximize its public health impact and should be investigated in future studies.

Several limitations should be acknowledged. First, the single-center retrospective design may limit generalizability to institutions with different patient populations, imaging protocols, or reader experience levels. Future multi-center studies incorporating diverse technical approaches would strengthen the evidence base for KS implementation. Second, the relatively limited number of non-mass lesions in our cohort may have reduced statistical power for detecting differences in this subgroup. Third, BPE was not evenly distributed across the study population, and the number of cases with marked BPE was insufficient for robust subgroup analysis. Fourth, while consensus reading strengthened the final MRI interpretations, the lack of individual reader data prevented inter-reader agreement analysis. Fifth, selection bias was present because only lesions identified as suspicious on ultrasound or mammography proceeded to MRI. This excluded subtler findings common in routine screening, constraining generalizability to varied clinical contexts and may inflate the diagnostic performance metrics, although this inclusion pattern is consistent with established practical medical workflow."

"Although our approach mirrors the clinical workflows but warrants caution in performance interpretation and validation in cohorts with uniform reference test confirmation.

CONCLUSION

Our study confirms the high diagnostic accuracy of the KS for breast MRI interpretation while demonstrating its superior specificity compared with conventional BI-RADS assessment. The integration of ADC values did not provide significant additional benefit, suggesting that the morphological and kinetic features encompassed by the KS adequately capture the essential diagnostic information for lesion characterization. The consistent performance across minimal, mild, and moderate BPE levels supports the clinical utility of this evidence-based diagnostic tool.

ETHICAL CONSIDERATIONS

We adhered to the ethical principles of the Declaration of Helsinki. This study was approved by the Institutional Review Board of Imam Khomeini Hospital Complex, and the requirement for written informed consent was waived.

DATA AVAILABILITY

The data supporting this article can be obtained from the corresponding author upon reasonable request.

CONFLICT OF INTERESTS

The authors declare no relevant financial or nonfinancial conflicts of interest.

FUNDING

This research received no specific grant from any funding agency in the public, commercial, or not-for-profit sectors.

ACKNOWLEDGMENTS

None.

AI DISCLOSURE

Artificial intelligence tools were used solely for language editing and stylistic improvement. All scientific content, data analysis, and interpretations were produced directly by the authors.

AUTHOR CONTRIBUTION

FZ: Conceptualization, Data curation, Formal analysis, Investigation, Methodology, Project administration, Supervision, Validation, Visualization, Writing – original draft, Writing – review & editing. PKH: Resources, Validation, Writing – review & editing. AM: Data curation, Formal analysis, Methodology, Visualization, Writing – original draft. ZS: Data curation. ZM: Data curation, Writing – original draft. FMS: Data curation, Writing – review & editing. AA: Data curation, Investigation, Writing – original draft. AHH: Data curation, Writing – review & editing. SB: Data curation, Writing – review & editing. HZ: Data curation, Writing – original draft. FA: Data curation, Writing – review & editing. FSK: Data curation, Visualization. SM: Conceptualization, Formal analysis, Methodology, Project administration, Resources, Software, Supervision, Validation, Writing – review & editing.

REFERENCES

1. Giaquinto AN, Sung H, Newman LA, Freedman RA, Smith RA, Star J, et al. Breast cancer statistics 2024. *CA: a cancer journal for clinicians.* 2024;74(6):477-95. doi: 10.3322/caac.21863.
2. 2. Bennani-Baiti B, Baltzer PA. MR Imaging for Diagnosis of Malignancy in Mammographic Microcalcifications: A Systematic Review and Meta-Analysis. *Radiology*. 2017;283(3):692-701. doi: 10.1148/radiol.2016161106.
3. 3. Mann RM, Kuhl CK, Kinkel K, Boetes C. Breast MRI: guidelines from the European Society of Breast Imaging. *European radiology.* 2008;18(7):1307-18. doi: 10.1007/s00330-008-0863-7.
4. Mann RM, Cho N, Moy L. Breast MRI: State of the Art. *Radiology*. 2019;292(3):520-36. doi: 10.1148/radiol.2019182947.
5. Nessim C, Winocour J, Holloway DP, Saskin R, Holloway CM. Wait times for breast cancer surgery: effect of magnetic resonance imaging and preoperative investigations on the diagnostic pathway. *Journal of oncology practice.* 2015;11(2):e131-8. doi: 10.1200/jop.2014.002105.
6. Purkayastha S, Zhao Y, Wu J, Hu R, McGirr A, Singh S, et al. Differentiation of low and high grade renal cell carcinoma on routine MRI with an externally validated automatic machine learning algorithm. *Scientific reports.* 2020;10(1):19503. doi: 10.1038/s41598-020-76132-z.
7. Strigel RM, Burnside ES, Elezaby M, Fowler AM, Kelcz F, Salkowski LR, et al. Utility of BI-RADS Assessment Category 4 Subdivisions for Screening Breast MRI. *AJR American journal of roentgenology*. 2017;208(6):1392-9. doi: 10.2214/ajr.16.16730.
8. Leithner D, Wengert G, Helbich T, Morris E, Pinker K. MRI in the Assessment of BI-RADS® 4 lesions. *Topics in magnetic resonance imaging : TMRI.* 2017;26(5):191-9. doi: 10.1097/rmr.0000000000000138.
9. Baltzer PA, Dietzel M, Kaiser WA. A simple and robust classification tree for differentiation between benign and malignant lesions in MR-mammography. *European radiology.* 2013;23(8):2051-60. doi: 10.1007/s00330-013-2804-3.
10. Istomin A, Masarwah A, Vanninen R, Okuma H, Sudah M. Diagnostic performance of the Kaiser score for characterizing lesions on breast MRI with comparison to a multiparametric classification system. *European journal of radiology.* 2021;138:109659. doi: 10.1016/j.ejrad.2021.109659.
11. Wang Q, Fu F, Chen Y, Yang D, Zhang J, Yu H, et al. Application of the Kaiser score by MRI in patients with breast lesions by ultrasound and mammography. *Diagnostic and interventional radiology (Ankara, Turkey).* 2022;28(4):322-8. doi: 10.5152/dir.2022.201075.
12. Dietzel M, Bernathova M, Clauser P, Kapetas P, Uder M, Baltzer PAT. Added value of clinical decision rules for the management of enhancing breast MRI lesions: A systematic comparison of the Kaiser score and the Göttingen score. *European journal of radiology.* 2023;169:111185. doi: 10.1016/j.ejrad.2023.111185.
13. Mohammadzadeh S, Mohebbi A, Moradi Z, Abdi A, Mohammadi A, Hakim PK, et al. Diagnostic performance of Kaiser score in the evaluation of breast cancer using MRI: A systematic review and meta-analysis. *European journal of radiology*. 2025;186:112055. doi: 10.1016/j.ejrad.2025.112055.
14. Zhang M, Horvat JV, Bernard-Davila B, Marino MA, Leithner D, Ochoa-Albiztegui RE, et al. Multiparametric MRI model with dynamic contrast-enhanced and diffusion-weighted imaging enables breast cancer diagnosis with high accuracy. *Journal of magnetic resonance imaging : JMRI*. 2019;49(3):864-74. doi: 10.1002/jmri.26285.
15. Baltzer A, Dietzel M, Kaiser CG, Baltzer PA. Combined reading of Contrast Enhanced and Diffusion Weighted Magnetic Resonance Imaging by using a simple sum score. *European radiology*. 2016;26(3):884-91. doi: 10.1007/s00330-015-3886-x.
16. Meng L, Zhao X, Lu L, Xing Q, Wang K, Guo Y, et al. A Comparative Assessment of MR BI-RADS 4 Breast Lesions With Kaiser Score and Apparent Diffusion Coefficient Value. *Frontiers in oncology*. 2021;11:779642. doi: 10.3389/fonc.2021.779642.
17. Pan J, Huang X, Yang S, Ouyang F, Ouyang L, Wang L, et al. The added value of apparent diffusion coefficient and microcalcifications to the Kaiser score in the evaluation of BI-RADS 4 lesions. *European journal of radiology*. 2023;165:110920. doi: 10.1016/j.ejrad.2023.110920.
18. Bechyna S, Baltzer PAT. Impact of Background Parenchymal Enhancement on Diagnostic Performance of Breast MRI: A Systematic Review and Meta-Analysis. *Radiology*. 2025;315(2):e241919. doi: 10.1148/radiol.241919.
19. Dietzel M, Baltzer PAT. How to use the Kaiser score as a clinical decision rule for diagnosis in multiparametric breast MRI: a pictorial essay. *Insights into imaging.* 2018;9(3):325-35. doi: 10.1007/s13244-018-0611-8.
20. Pötsch N, Vatteroni G, Clauser P, Helbich TH, Baltzer PAT. Contrast-enhanced Mammography versus Contrast-enhanced Breast MRI: A Systematic Review and Meta-Analysis. *Radiology*. 2022;305(1):94-103. doi: 10.1148/radiol.212530.
21. Su X, Wang S. Is Magnetic Resonance Imaging (MRI) Still a Gold Standard to Detect Breast Cancer: A Meta-analysis. *Current medical imaging.* 2023;19(14):1643-55. doi: 10.2174/1573405619666230206162504.
22. Baltzer PAT, Krug KB, Dietzel M. Evidence-Based and Structured Diagnosis in Breast MRI using the Kaiser Score. *RoFo : Fortschritte auf dem Gebiete der Rontgenstrahlen und der Nuklearmedizin.* 2022;194(11):1216-28. doi: 10.1055/a-1829-5985.
23. Ostillio E, Carriero S, Razzini D, Groenhoff L, Tambasco A, Airoldi C, et al. Diagnostic Performance

of Kaiser score in MRI BI-RADS 3 Lesions: A Promising tool to reduce unnecessary biopsies. *European journal of radiology.* 2025;183:111872. doi: 10.1016/j.ejrad.2024.111872.
24. Clauser P, Krug B, Bickel H, Dietzel M, Pinker K, Neuhaus VF, et al. Diffusion-weighted Imaging Allows for Downgrading MR BI-RADS 4 Lesions in Contrast-enhanced MRI of the Breast to Avoid Unnecessary Biopsy. *Clinical cancer research : an official journal of the American Association for Cancer Research.* 2021;27(7):1941-8. doi: 10.1158/1078-0432.ccr-20-3037.
25. Zhang J, Li L, Zhang L, Zhe X, Tang M, Lei X, et al. Meta-analysis of dynamic contrast enhancement and diffusion-weighted MRI for differentiation of benign from malignant non-mass enhancement breast lesions. *Frontiers in oncology*. 2024;14:1332783. doi: 10.3389/fonc.2024.1332783.
26. Dietzel M, Vatteroni G, Baltzer PAT. What Is the Added Value of DWI Compared With Structured Assessment of BI-RADS Criteria by the Kaiser Score? A Systematic Review and Meta-analysis. *Investigative radiology.* 2025;60(3):175-83. doi: 10.1097/rli.0000000000001123.
27. Youn I, Biswas D, Hippe DS, Winter AM, Kazerouni AS, Javid SH, et al. Diagnostic Performance of Point-of-Care Apparent Diffusion Coefficient Measures to Reduce Biopsy in Breast Lesions at MRI: Clinical Validation. *Radiology*. 2024;310(2):e232313. doi: 10.1148/radiol.232313.
28. Penn A, Medved M, Abe H, Dialani V, Karczmar GS, Brousseau D. Safely reducing unnecessary benign breast biopsies by applying non-mass and DWI directional variance filters to ADC thresholding. *BMC medical imaging.* 2022;22(1):171. doi: 10.1186/s12880-022-00897-0.
29. Partridge SC, DeMartini WB, Kurland BF, Eby PR, White SW, Lehman CD. Quantitative diffusion-weighted imaging as an adjunct to conventional breast MRI for improved positive predictive value. *AJR American journal of roentgenology.* 2009;193(6):1716-22. doi: 10.2214/ajr.08.2139.
30. Duijm LEM. Dense breasts at breast cancer screening: can DWI-based breast MRI without contrast help us in the pursuit of personalized screening? *European radiology.* 2024;34(7):4727-9. doi: 10.1007/s00330-023-10323-w.
31. Arian A, Teymouri Athar MM, Nouri S, Ghorani H, Khalaj F, Hejazian SS, et al. Role of breast MRI BI-RADS descriptors in discrimination of non-mass enhancement lesion: A systematic review & meta-analysis. *European journal of radiology*. 2025;185:111996. doi: 10.1016/j.ejrad.2025.111996.
32. Newell D, Nie K, Chen JH, Hsu CC, Yu HJ, Nalcioglu O, et al. Selection of diagnostic features on breast MRI to differentiate between malignant and benign lesions using computer-aided diagnosis: differences in lesions presenting as mass and non-mass-like enhancement. *European radiology.* 2010;20(4):771-81. doi: 10.1007/s00330-009-1616-y.
33. Jansen SA, Shimauchi A, Zak L, Fan X, Karczmar GS, Newstead GM. The diverse pathology and kinetics of mass, nonmass, and focus enhancement on MR imaging of the breast. *Journal of magnetic resonance imaging : JMRI.* 2011;33(6):1382-9. doi: 10.1002/jmri.22567.
34. Liu G, Li Y, Chen SL, Chen Q. Non-mass enhancement breast lesions: MRI findings and associations with malignancy. *Annals of translational medicine*. 2022;10(6):357. doi: 10.21037/atm-22-503.
35. Brooks JD, Christensen RAG, Sung JS, Pike MC, Orlow I, Bernstein JL, et al. MRI background parenchymal enhancement, breast density and breast cancer risk factors: A cross-sectional study in pre- and post-menopausal women. *NPJ breast cancer*. 2022;8(1):97. doi: 10.1038/s41523-022-00458-2.
36. Liao GJ, Henze Bancroft LC, Strigel RM, Chitalia RD, Kontos D, Moy L, et al. Background parenchymal enhancement on breast MRI: A comprehensive review. *Journal of magnetic resonance imaging : JMRI*. 2020;51(1):43-61. doi: 10.1002/jmri.26762.
37. Zhou XZ, Liu LH, He S, Yao HF, Chen LP, Deng C, et al. Diagnostic value of Kaiser score combined with breast vascular assessment from breast MRI for the characterization of breast lesions. *Frontiers in oncology.* 2023;13:1165405. doi: 10.3389/fonc.2023.1165405.
38. Kuhl CK. Abbreviated Breast MRI: State of the Art. *Radiology*. 2024;310(3):e221822. doi: 10.1148/radiol.221822.
39. Kim JM, Ha SM. Clinical Application of Artificial Intelligence in Breast MRI. *Journal of the Korean Society of Radiology.* 2025;86(2):227-35. doi: 10.3348/jksr.2025.0012.

How to Cite This Article

Oliveira PSD, Andréa LSP, da Silva AV, Aguiar-Alves F. The TP53 p.R337H Variant in Breast Cancer: Evidence from a Cohort Study and Literature Review. Arch Breast Cancer. 2026; 13(3):359-372.
Available from: https://www.archbreastcancer.com/index.php/abc/article/view/1299